Short-interfering RNAs Induce Retinal Degeneration via TLR3 and IRF3

Mark E Kleinman[1], Hiroki Kaneko[1], Won Gil Cho[1,2], Sami Dridi[1], Benjamin J Fowler[1], Alexander D Blandford[1], Romulo JC Albuquerque[1], Yoshio Hirano[1], Hiroko Terasaki[3], Mineo Kondo[4], Takashi Fujita[5], Balamurali K Ambati[6,7], Valeria Tarallo[1], Bradley D Gelfand[1], Sasha Bogdanovich[1], Judit Z Baffi[1] and Jayakrishna Ambati[1,8]

[1]Department of Ophthalmology and Visual Sciences, University of Kentucky, Lexington, Kentucky, USA; [2]Department of Anatomy, Yonsei University Wonju College of Medicine, Wonju City, Korea; [3]Department of Ophthalmology, Nagoya University Graduate School of Medicine, Nagoya, Japan; [4]Department of Ophthalmology, Mie University Graduate School of Medicine, Tsu, Japan; [5]Department of Molecular Genetics, Institute for Virus Research, and Graduate School of Biostudies, Kyoto University, Kyoto, Japan; [6]Department of Ophthalmology and Visual Sciences, Moran Eye Center, University of Utah School of Medicine, Salt Lake City, Utah, USA; [7]Department of Ophthalmology, Veterans Affairs Salt Lake City Healthcare System, Salt Lake City, Utah, USA [8]Department of Physiology, University of Kentucky, Lexington, Kentucky, USA

The discovery of sequence-specific gene silencing by endogenous double-stranded RNAs (dsRNA) has propelled synthetic short-interfering RNAs (siRNAs) to the forefront of targeted pharmaceutical engineering. The first clinical trials utilized 21-nucleotide (nt) siRNAs for the treatment of neovascular age-related macular degeneration (AMD). Surprisingly, these compounds were not formulated for cell permeation, which is required for bona fide RNA interference (RNAi). We showed that these "naked" siRNAs suppress neovascularization in mice not via RNAi but via sequence-independent activation of cell surface Toll-like receptor-3 (TLR3). Here, we demonstrate that noninternalized siRNAs induce retinal degeneration in mice by activating surface TLR3 on retinal pigmented epithelial cells. Cholesterol conjugated siRNAs capable of cell permeation and triggering RNAi also induce the same phenotype. Retinal degeneration was not observed after treatment with siRNAs shorter than 21-nts. Other cytosolic dsRNA sensors are not critical to this response. TLR3 activation triggers caspase-3-mediated apoptotic death of the retinal pigment epithelium (RPE) via nuclear translocation of interferon regulatory factor-3. While this unexpected adverse effect of siRNAs has implications for future clinical trials, these findings also introduce a new preclinical model of geographic atrophy (GA), a late stage of dry AMD that causes blindness in millions worldwide.

Received 24 July 2011; accepted 12 September 2011; published online 11 October 2011. doi:10.1038/mt.2011.212

INTRODUCTION

Significant vision loss from age-related macular degeneration (AMD) is most commonly due to pathologic choroidal neovascularization, vascular leakage, and subsequent fluid accumulation in the neurosensory retina. This disease process disrupts the delicate interface between photoreceptors and the underlying retinal pigment epithelium (RPE), an intercellular array that is essential for optimal vision. Pharmacologic inhibition of vascular endothelial growth factor-A using targeted monoclonal antibody therapy has become the mainstay of treatment for this blinding disease with excellent efficacy. Several other modalities of vascular endothelial growth factor-A targeted therapies have been investigated including post-transcription gene silencing via short-interfering RNAs (siRNAs), an approach that showed great promise in preclinical studies. However, the two pioneering clinical trials studying the first generation of siRNA-based drugs targeting vascular endothelial growth factor-A in the treatment of neovascular AMD were abruptly halted because they failed to reach primary endpoints. Published data from one of these trials reported some efficacy with lower but not high-range doses.[1] While these studies were underway, we reported the surprising discovery that 21-nucleotide (nt) siRNA duplexes, the standard length for clinically translated RNA interference (RNAi) therapeutics including those utilized in the vascular endothelial growth factor-A studies, activated the innate immune receptor Toll-like receptor 3 (TLR3) independent of sequence or target.[2] Recently, independent reports have similarly confirmed that 21-nt siRNAs, including control sequences, decrease endothelial cell proliferation and suppress angiogenesis *in vivo*.[3–5]

TLRs are type I transmembrane proteins that recognize pathogen-associated molecular patterns resulting in the initiation of the innate immune response and interferon pathways. To date, 10 functional TLRs have been identified in humans that bind with specific pathogen-associated molecular patterns present in many infectious elements. Viral double-stranded RNA (dsRNA) has long been known to induce a cytotoxic response, yet it is only within the past decade that this mechanism was shown to be partly mediated by specific recognition of dsRNA through TLR3,[6] which is expressed almost ubiquitously throughout most tissues including specialized ocular cell types.[7] Further studies revealed the critical

M.E.K., H.K., and W.G.C. contributed equally to this work.

Correspondence: *Jayakrishna Ambati, Department of Ophthalmology and Visual Sciences, University of Kentucky, 740 S. Limestone Street, Ste E302, Lexington, Kentucky 40536-0284, USA. E-mail: jamba2@email.uky.edu*

involvement of an intracytosolic protein called Toll/IL-1 receptor domain-containing adapter inducing interferon-β (TRIF)[8,9] which can relay TLR3 activation through nuclear factor-κB and interferon regulatory factor-3.[10] This divergent signaling pathway may be important in controlling immune-mediated cell-type and condition specific responses to TLR3 activation through selective induction of interferon-related and cytokine gene cassettes.

Redundant mechanisms have evolved to ensure an accurate and sensitive detection of nonself dsRNA during mammalian immune surveillance. In addition to TLR3, there are other known dsRNA receptors including RNA-binding protein kinase (PKR), retinoic acid inducible gene I (RIG-I), and melanoma differentiation-associated gene 5 (MDA5). RIG-I recognizes RNA of various lengths with 5′-triphosphates and some partial double-stranded characteristics whereas MDA5 senses very long dsRNA molecules (>2,000-nt).[11,12] Exposure to long dsRNA (>40-nt) results in robust TLR3 signaling via multimerization of the ligand bound extracellular domains, however 21-nt siRNA can also activate TLR3.[13,14] Collectively, these data suggest that the cellular effects of targeted 21-nt siRNA are not limited to gene silencing and may induce unexpected cytotoxicity via TLR3 activation and its downstream signaling components.

We previously demonstrated that poly I:C (pIC), a synthetic high-molecular weight dsRNA that is internalized by cells[15] and activates TLR3[6] and other dsRNA sensors,[16] induced significant retinal degeneration with large areas of RPE cell loss and apoptosis of adjacent photoreceptors.[17] In the present study, we investigated the effects of intraocular administration of 21-nt siRNA on the retina and observed an acute cytotoxic response with significant RPE degeneration that was dependent on TLR3 and its downstream transcription factor, interferon regulatory factor-3. Shortening the siRNA duplex to 16-nt, which is a nonactivating TLR3 ligand, significantly reduced cytotoxicity suggesting that future intraocular RNAi therapeutic development should consider similarly shortened siRNA designs.

RESULTS

Short and long dsRNAs induce retinal degeneration

Intravitreous administration of chemically unmodified 21-nt-siRNAs (2 µg) which are not formulated for cell permeation and similar to those used in the clinical trials for AMD uniformly induced retinal toxicity resulting in large areas of significant RPE cell loss and degeneration at 1 week after treatment compared to vehicle control (**Figure 1a,b**). This effect was observed at concentrations equivalent to those used in the higher doses of the previously mentioned clinical trials (0.3–0.4 µg/µl) as calculated by comparison of siRNA dosage and mouse and human vitreous volumes (~7 µl and 4 ml with doses of 2 µg and 1,200 or 1,600 µg, respectively). Conversely, a 16-nt siRNA targeting firefly luciferase (14-nt long RNA duplex with 2-nt overhangs, 16-nt-*Luc*-siRNA) that does not activate TLR3[2,14] was not toxic to the retina at equimolar concentrations (**Figure 1c**). *In vivo* imaging using spectral domain optical coherence tomography revealed significant disruption of the outer retina consistent with acute damage to the RPE and photoreceptor layers (**Figure 1d**).

Long dsRNA including pIC and poly I:C_{12}U (Ampligen), a more specific activator of TLR3 than pIC,[18] had similar effects on the retina (**Supplementary Figure S1a**). Moreover, we found that retinal degeneration induced by 21-nt siRNA was independent of target or sequence, as several other unmodified siRNAs including duplexes identical in sequence to those studied in clinical trials exhibited similar effects (**Supplementary Figure S1b** and **Supplementary Table S1** for sequences). Conjugation of 21-nt siRNAs to cholesterol, which enables cell permeation and thus bona fide RNAi,[19] also caused retinal degeneration (**Supplementary Figure S2**). Interestingly, no retinal degeneration occurred after repeated administration of high-dose intravenous serum stable 21-nt-*Luc*-siRNA (**Supplementary Figure S3**) suggesting that 21-nt-siRNA does not efficiently penetrate the outer blood–retina barrier.

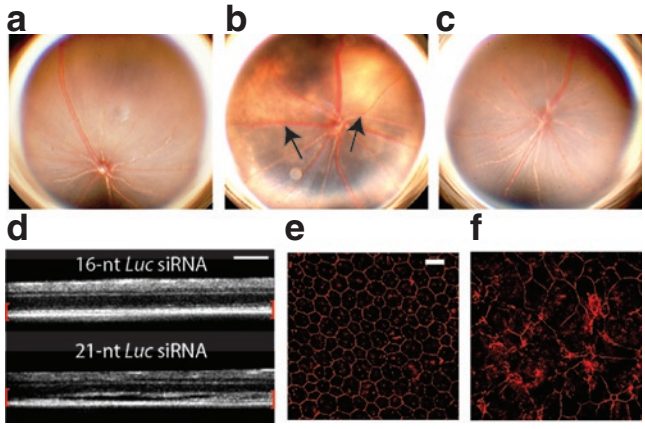

Figure 1 21-Nucleotide (nt) short-interfering RNAs (siRNAs) induce retinal degeneration. (**a**) Representative fundus photographs of mice 7 days after treatment with intravitreous phosphate-buffered saline (PBS) control and (**b**) 21-nt-*Luc*-siRNA demonstrating large hypopigmented areas indicative of retinal pigment epithelium (RPE) loss (black arrows, $n = 24$ per group in four independent experiments, $P < 0.0001$ by Fisher's exact test). (**c**) Administration of 16-nt-*Luc*-siRNA did not induce retinal degeneration ($n = 24$ in four independent experiments, $P < 0.0001$). (**d**) *In vivo* retinal imaging with optical coherence tomography revealed marked disruption of the outer retina and RPE (enclosed in red brackets) with 21-nt *Luc* siRNA ($n = 6$ in two independent experiments). Zonula occludens-1 (ZO-1) immunofluorescence (red) of RPE flat mounts 1 week after 16-nt-*Luc*-siRNA (**e**) showed uniformly arranged hexagonal cells, but 21-nt-*Luc*-siRNA treatment (**f**) resulted in significant disruption of this junctional pattern with large variations in cellular morphology ($n = 4$ in two independent experiments). Bars (d) = 200 µm; Bars (e, f) = 20 µm.

Disruption of the RPE after intraocular dsRNA

RPE function is vital for the regulation of photoreceptor renewal and maintenance of the outer blood retina barrier both of which are essential for optimal vision. We found that 21-nt-*Luc*-siRNA-induced significant disruptions of RPE cell–cell junctions as visualized on flat mounts by zonula occludens-1 immunofluorescence whereas 16-nt-*Luc*-siRNA did not alter the hexagonal tessellation of the RPE monolayer (**Figure 1e**). Similarly, globally expressing enhanced green fluorescent protein mice exhibited decreased enhanced green fluorescent protein signal in RPE and nuclear fragmentation consistent with cell death after treatment with 21-nt-*Luc*-siRNA (**Supplementary Figure S4**). Histomorphologic analyses revealed RPE cell damage with severe vacuolization and pigment loss compared to mouse eyes treated with vehicle control (**Figure 2a,b**). Ultrastructural studies demonstrated normal appearing cells in vehicle and 16-nt-*Luc*-siRNA-treated mouse eyes (**Figure 2c,d**), but pyknotic nuclei and phagocytic bodies in RPE cells were abundant with disorganization of the overlying photoreceptor array in

the 21-nt-*Luc*-siRNA group (**Figure 2e**). Global retinal function as quantified by scotopic flash electroretinography was significantly diminished after intravitreous injections of 21-nt-*Luc*-siRNA (**Figure 3**). Collectively, these data suggest that both short and long dsRNAs induce acute and severe RPE cytotoxicity resulting in loss of trophic support at the photoreceptor interface, decreased visual function and fundoscopic changes similar to the advanced form of dry AMD known as geographic atrophy (GA).[20]

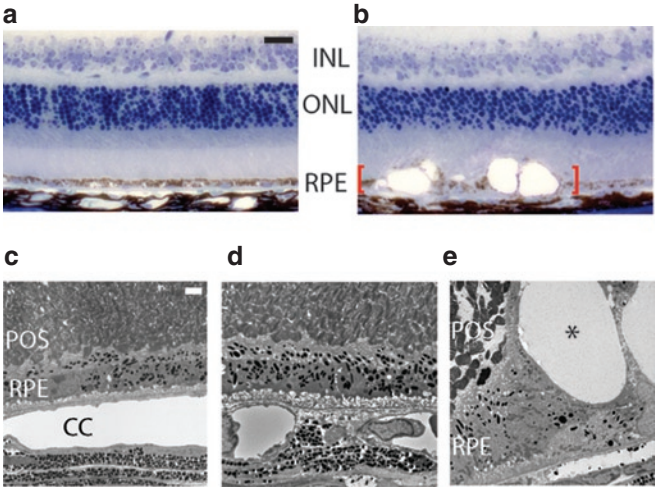

Figure 2 Microscopic features of 21-nucleotide (nt) short-interfering RNAs (siRNAs) induced retinal degeneration. Histomorphologic assessment at 1 week after treatment (n = 6–8 in two independent experiments) showed that (**a**) 16-nt-*Luc*-siRNA did not change normal appearing RPE cell monolayer, whereas (**b**) 21-nt-*Luc*-siRNA resulted in marked retina and RPE degeneration with severe pigment loss and vacuolization (red brackets). Ultrastructural examination at this time-point (n = 4–6 in two independent experiments) revealed an orderly photoreceptor array and confluent RPE in phosphate-buffered saline (PBS) and 16-nt-*Luc*-siRNA (**c**, **d**) but significant alterations of the RPE with large vacuoles (asterisk) with 21-nt-*Luc*-siRNA (**e**). Bars (a–b) = 20 µm; (c–e), 2 µm. INL, inner nuclear layer; ONL, outer nuclear layer; POS, photoreceptor outer segments, RPE, retinal pigment epithelium.

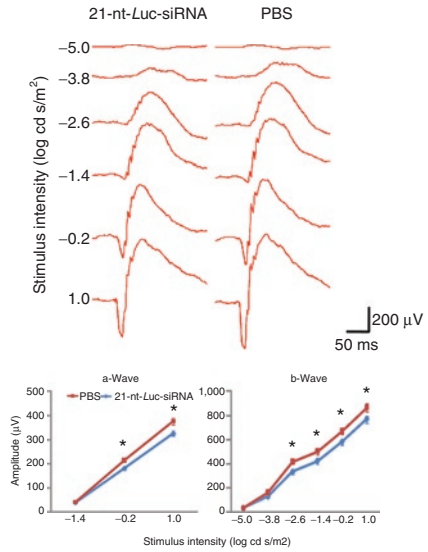

Figure 3 Intravitreous 21-nucleotide (nt)-short-interfering RNA (siRNA) administration suppresses retinal function. Representative wave form and amplitude responses during scotopic flash electroretinography (ERG) in mice are shown. Weekly intravitreous administration of 21-nt-*Luc*-siRNA for a total of three injections resulted in significant decrease of the a- and b-wave amplitude responses by 15.8 ± 0.87% and 13.2 ± 0.39%, respectively, compared to phosphate-buffered saline (PBS) control (n = 8 per group in two independent experiments, *P < 0.05, Mann–Whitney U test).

21-nt siRNA-induced retinal degeneration requires TLR3

The mammalian immune system has multiple receptors capable of dsRNA recognition, so we rigorously studied various animal models to determine which of them are required to induce this phenotype. We observed that 21-nt-*Luc*-siRNA did not result in retinotoxicity in wild-type mice when coadministered with TLR3 neutralizing antibodies [compared to equimolar immunoglobulin G (IgG) control] or in TLR3-deficient mice (**Figure 4a–c**). We then tested whether activation of other cytoplasmic dsRNA sensors including RIG-I, MDA-5, and PKR were required for this class effect. Whereas wild-type mice treated with the RIG-I-specific ligand 3p-RNA[12] showed no evidence of retinal toxicity (**Supplementary Figure S5**), and both *Mda5*$^{-/-}$ and *Pkr*$^{-/-}$ mice treated with intravitreous pIC developed retinal degeneration similar to wild-type mice (**Supplementary Figure S6**).

TLR3 is expressed on the cell surface and interacts with 21-nt siRNA in RPE

Although TLR3 expression was initially identified in intracellular endosome-like compartments,[21] recent data demonstrate its expression on the surface of many cell types.[2,22,23] Firstly, we observed

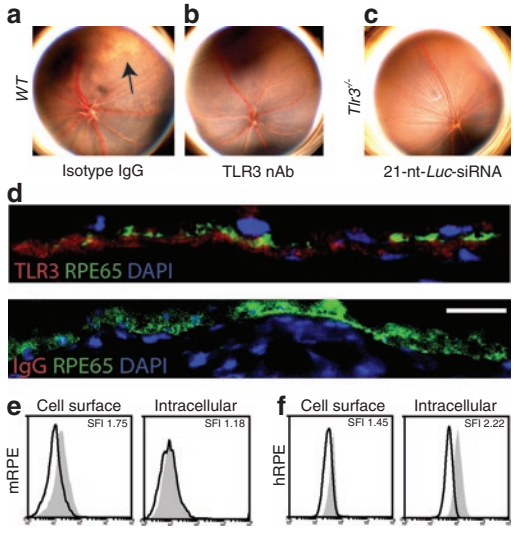

Figure 4 Short and long double-stranded RNA (dsRNA) induced retinal degeneration requires Toll-like receptor-3 (TLR3). (**a**) A representative color fundus photograph showing retinal degeneration after intravitreous coadministration of 21-nt-*Luc*-siRNA and isotype immunoglobulin G (IgG) (n = 6 in two independent experiments). (**b**, **c**) 21-nt-*Luc*-siRNA-induced retinal toxicity did not occur when eyes were pretreated with neutralizing TLR3 antibodies (n = 6 in two independent experiments) or in mice deficient in TLR3 expression (*Tlr3*$^{-/-}$, n = 12 in three independent experiments). (**d**) TLR3 immunofluorescence in mouse eyes show strong signal colocalization with the retinal pigment epithelium (RPE) marker, RPE65 (n = 3 in three independent experiments, Bar = 10 µm). Representative histograms of cell surface and intracellular TLR3 staining in mouse RPE (mRPE) (**e**) and human RPE (hRPE) (**f**) cells (n = 4–5 in two independent experiments). nt, nucleotide.

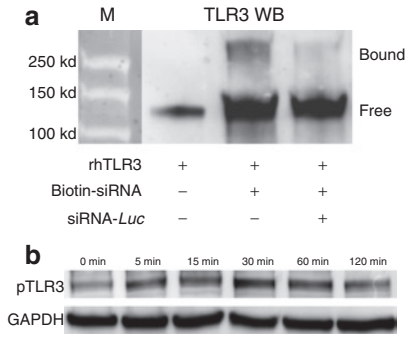

Figure 5 21-Nucleotide (nt) short-interfering RNA (siRNA) binds to and activates Toll-like receptor-3 (TLR3) expressed on the retinal pigment epithelium (RPE) cell surface. (**a**) Physical binding was confirmed on avidin immunoprecipitation of biotinylated 21-nt *Luc* siRNA which showed a >250 kDa TLR3 immunoreactive band that was reduced by competition assay ($n = 3$ in three independent experiments). (**b**) TLR3 phosphorylation was detected in primary hRPE cells as early as 5 minutes after exposure to 21-nt-*Luc*-siRNA ($n = 3$ in three independent experiments). GAPDH served as loading control.

strong TLR3 expression immunolocalized to RPE with a cell-specific marker, RPE65, in untreated mouse eye sections (**Figure 4d**). Using flow cytometry, surface and intracellular localization of TLR3 was confirmed in mouse and human RPE cells (mRPE and hRPE, respectively), suggesting that these cells were susceptible to immune activation by both extracellular and cell-permeant 21-nt-siRNA (**Figure 4e,f**). Previous data strongly suggests that 21-nt-siRNA physically interacts with and activates TLR3,[2,14,24] but conclusive evidence of this has been difficult to obtain. Thus, we performed competitive binding assays and phosphorylation studies to investigate this further. Indeed, we observed biochemical evidence of binding between a purified recombinant human TLR3 ectodomain and biotinylated 21-nt-*Luc*-siRNA along with receptor dimerization (**Figure 5a**), a process that is required for TLR3 activation.[25] The specificity of TLR3 binding was confirmed with competition assays using excess unmodified 21-nt-*Luc*-siRNA. In addition to binding 21-nt-*Luc*-siRNA, we also show that exposure of hRPE cells to noncell-permeant 21-nt-*Luc*-siRNA induces rapid TLR3 phosphorylation (**Figure 5b**). These data support a model in which extracellular 21-nt siRNA can bind to TLR3 and initiate its intracytosolic signaling cascade.[26]

TLR3 activation results in cell death and cleavage of caspase-3 in the retinal pigment epithelium

While numerous mechanisms may lead RPE loss after dsRNA treatment, TLR3 activation is a well-established and potent proapoptotic stimulus in numerous cell types including RPE.[17,27,28] In this study, hRPE cells treated with pIC or 21-nt-*Luc*-siRNA exhibited significantly decreased proliferation *in vitro* compared to 16-nt-*Luc*-siRNA (**Figure 6a**). TUNEL staining identified increased late apoptotic cells in eyes treated with 21-nt-*Luc*-siRNA but not 16-nt-*Luc*-siRNA, especially in areas of outer nuclear layer with wave-like features (**Figure 6b,c**), a specific finding previously reported in other animal models of retinal degeneration.[29] Many studies indicate that TLR3-mediated apoptosis occurs through caspase-dependent pathways.[30–32] We found that intravitreous injection of 21-nt-*Luc*-siRNA and pIC induced significant caspase-3 cleavage in

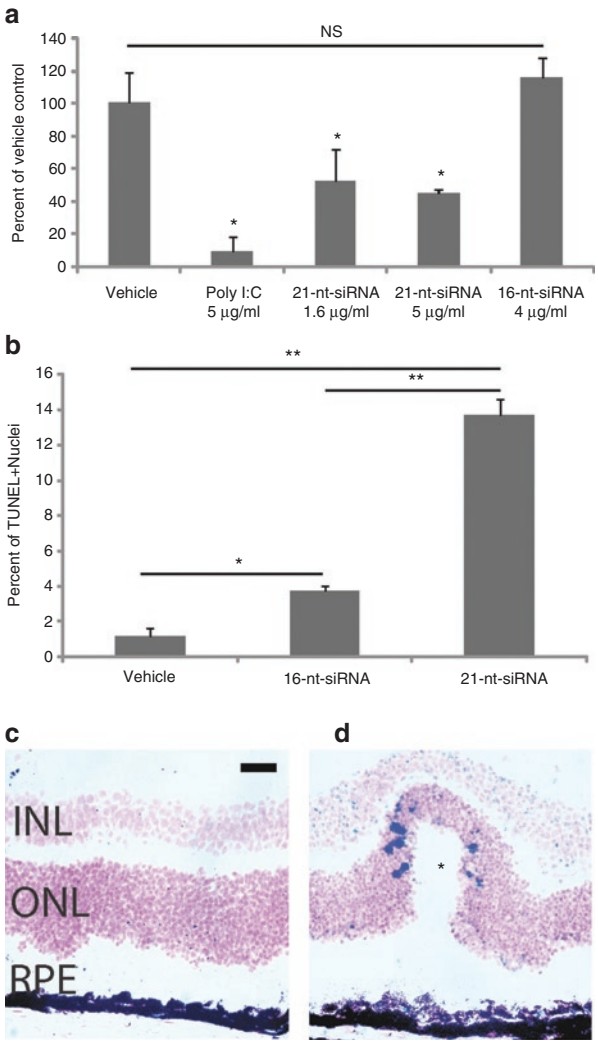

Figure 6 21-Nucleotide (nt) short-interfering RNA (siRNA) reduces retinal pigment epithelium (RPE) viability and increases apoptosis. (**a**) Both poly I:C (pIC) and 21-nt-*Luc*-siRNA significantly decreased hRPE cell proliferation as measured by BrdU incorporation ($n = 3$ in three independent experiments). (**b**, **c**) TUNEL staining identified significantly increased numbers of late apoptotic cells in the retina and RPE layers in 21-nt-*Luc*-siRNA compared to 16-nt-*Luc*-siRNA at 24 hours ($n = 6$ in two independent experiments, 13.68 ± 0.89% vs. 3.70 ± 0.25%, $P < 0.01$, Mann–Whitney *U*-test). TUNEL+ nuclei were more heavily concentrated in areas of wave-like changes in the ONL/RPE (asterisk). $^{**}P < 0.01$ and $^{*}P < 0.05$ by Mann–Whitney *U*-test. Bars represent means ± SEM. Bar = 20 µm.

mouse RPE using both a substrate-dependent quantitative fluorometric assay and immunohistochemistry technique (**Figure 7a–d**). Caspase-3 activation was less robust although significantly elevated in hRPE cell cultures treated with 21-nt-*Luc*-siRNA or pIC (1.14 ± 0.11, $P = 0.07$ and 1.19 ± 0.085-fold compared to vehicle control, respectively, $P < 0.05$). These data support a model of caspase-dependent RPE apoptosis after 21-nt-*Luc*-siRNA exposure.

TLR3 signaling in RPE is routed via the transcription factor IRF3

TLR3 is the only member of the TLR family that is solely dependent on the intracytosolic adaptor TIR domain-containing adapter inducing interferon-β (TRIF).[10] While TLR4-mediated signaling is

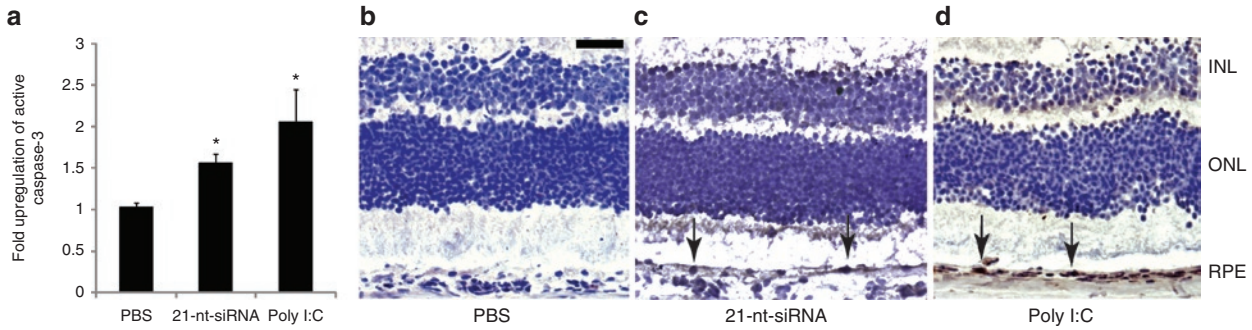

Figure 7 21-Nucleotide (nt) short-interfering RNA (siRNA)-induced Toll-like receptor-3 (TLR3) signaling activates caspase-3 in retinal pigment epithelium (RPE). (**a**) Active cleaved caspase-3 was quantified by fluorometric assay in mouse RPE/choroid and hRPE cells after treatment with 21-nt-*Luc*-siRNA and poly I:C (pIC) compared to phosphate-buffered saline (PBS) control ($n = 6$ in two independent experiments, fold-upregulation 1.56 ± 0.11 and 2.05 ± 0.39, respectively). (**b**–**d**) Immunodetection of active cleaved caspase-3 in albino Balb/C mouse eyes 24 hours after 21-nt-*Luc*-siRNA or pIC showed increased signal in RPE cells (black arrows) and variable staining in the neural retinal layers ($n = 3$ in three independent experiments, Bar = 20 µm). *$P < 0.05$ by Mann–Whitney *U*-test. Bars represent means ± SEM. siRNA, short-interfering RNA.

able to relay via TRIF or MyD88,[8] we did not observe acute RPE cell loss in wild-type mice after with intravitreous lipopolysaccharide (250 ng and 1 µg, data not shown). TRIF signaling bifurcates via nuclear translocation of either IRF3 or nuclear factor-κB. Previously, we reported that sequence and target independent suppression of choroidal neovascularization by 21-nt-siRNA was dependent on TRIF and downstream nuclear factor-κB signaling.[2] Conversely, in the current model, we found no evidence of retinal degeneration in *Irf3*$^{-/-}$ mice treated with intravitreous administration of vehicle control, 21-nt-*Luc*-siRNA or pIC (**Figure 8a–c**). Histomorphologic, ultrastructural, and electroretinography analyses were similar between the control treatments in wild-type mice and pIC treatments in *Irf3*$^{-/-}$ mice (**Supplementary Figure S7a–f**). In 21-nt-*Luc*-siRNA-treated hRPE cell cultures, we confirmed increased nuclear translocation of IRF3 compared to vehicle control (**Figure 8d**). These data implicate IRF3 translocation as a critical signaling event for 21-nt-siRNA-induced retinal degeneration.

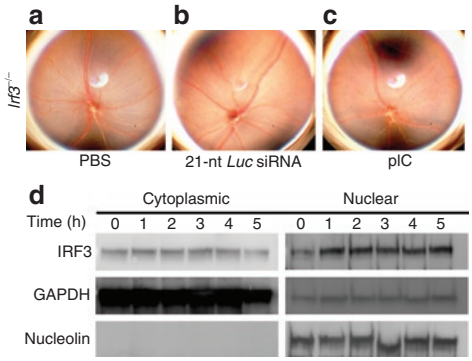

Figure 8 Toll-like receptor-3 (TLR3)-mediated retinal pigment epithelium (RPE) cell death signals via IRF3. (**a**–**c**) *Irf3*$^{-/-}$ mice did not exhibit fundus changes with 21-nt-*Luc*-siRNA. (**d**) IRF3 immunoblots of cytoplasmic and nuclear fractions showed increased nuclear signal in hRPE cells 1 hour after treatment with 21-nt-*Luc*-siRNA ($n = 3$ in three independent experiments). Housekeeping proteins GAPDH and nucleolin served as loading controls for cytoplasmic and nuclear fractions, respectively. nt, nucleotide. siRNA, short-interfering RNA.

DISCUSSION

While RNAi technology remains a promising modality for future gene targeted therapeutics, this study provides further evidence of the potential unanticipated side effects associated with the intraocular use of 21-nt-siRNA. Administration of doses equivalent to those given in human clinical trials in a mouse model resulted in significant retinotoxicity with widespread disruption of the RPE and loss of retinal function. With only a single report published with data from the clinical trials that provided no detailed anatomical descriptions or photographic documentation of treated eyes,[1] it is difficult to determine whether similar effects on the RPE were observed in the study patients. However, choroidal neovascularization due to neovascular AMD can often progress to RPE atrophy thus masking the possible deleterious effects of 21-nt-siRNA on the RPE. Collectively, our data strongly suggest that the intraocular use of siRNA-based drugs undergo careful re-evaluation, as unintended immune side effects likely extend beyond our previous findings of neovascular suppression[2] to initiation of inflammatory and proapoptotic signaling pathways in multiple cell types in the eye. With further optimization and more rigorous studies, siRNA modifications, both chemical and structural, may mitigate the inherent immunostimulatory properties of this pharmacologic approach thereby allowing its safe use in vision threatening eye diseases. Several findings observed in this study may help yield such a potential novel drug design.

Firstly, we were able to identify specific critical mediators of dsRNA-induced retinotoxicity. The induction of apoptosis in RPE via dsRNA required TLR3 and the transcription factor, IRF3. Moreover, the process may be caspase dependent. Concomitant TLR3 blockade with siRNA administration protected mouse eyes from retinotoxic side-effect suggesting that a similar strategy may be possible in human eyes. Another approach would be to simply shorten the siRNA duplex, as we did not detect retinal toxicity with 16-nt siRNAs. Our data suggest that evasion of immune system recognition may be accomplished by the use of shorter than 21-nt-siRNA duplexes, which we term ultrashort-interfering RNA (usi-RNA). Concerns remain about achieving efficient RNAi with usi-RNA, yet they have been successfully engineering and utilized without evidence of TLR3 or interferon activation.[33] We are currently studying these shortened duplexes, their targeting efficiency and *in vivo* stability in well-established mouse models of choroidal neovascularization. Additionally, viral delivery of siRNA (or short-hairpin RNA) via gene therapy remains a potentially viable option.

Lastly, it is of great interest that dsRNA-induced RPE toxicity resembles the advanced dry form of AMD, GA, a blinding eye disease affecting millions of people worldwide with no effective treatment. Previous studies suggest that there is an initial insult to the RPE followed by degeneration of the underlying choriocapillaris during the pathogenesis of GA.[34] From our previous work, we know that these dsRNAs result in death of choroidal endothelial cells, as they too express surface TLR3.[2] In this study, there was significant disruption of the RPE and photoreceptor layers, but apoptosis was also observed in the choroidal vasculature. Thus, this animal model of dsRNA-induced RPE degeneration may provide an avenue to explore the pathogenesis of GA. Indeed, we recently discovered increased concentrations of dsRNA derived from *Alu* repetitive sequences in RPE/choroid in affected eyes[35] and are currently studying which proapoptotic pathways are activated in short, long, and *Alu*-derived dsRNA-induced retinotoxicity. Ultimately, these data may expedite the search for safe and effective RNAi therapeutics and yield crucial insights into the pathobiology of a common age-related disease.

MATERIALS AND METHODS

Animals. All animal experiments were approved by institutional review committees and the Association for Research in Vision and Ophthalmology. C57Bl/6J, C57-eGFP, and *Tlr3*$^{-/-}$ mice were purchased from The Jackson Laboratory, Bar Harbor, ME. Transgenic mice deficient in *Irf3*$^{-/-}$ (gift of T. Taniguchi via M. David), *Pkr*$^{-/-}$ (gift of R.H. Silverman via G. Luo) and *Mda5*$^{-/-}$ (gift of M. Colonna) have all been previously described. For all procedures, mice were anesthetized by intraperitoneal injection of ketamine (50 mg/kg; Ft. Dodge Animal Health, Ft Dodge, IA) and xylazine (10 mg/kg; Phoenix Scientific, St Joseph, MO), and pupils were dilated with topical tropicamide (1%; Alcon Laboratories, Ft Worth, TX).

Human RPE cell isolates. Primary human RPE (hRPE) cell isolates (gift of D.R. Hinton) were genotyped for known TLR3 polymorphisms and used at low passage (3–6). Cells were cultivated in Dulbecco's modified Eagle's medium (high-glucose) with 10% fetal bovine serum (Gibco, Carlsbad, CA) and antibiotics. Prior to treatment with dsRNA, hRPE isolates were pretreated with interferon-α/β (1,000 U/ml, PBL InterferonSource, Piscataway, NJ) for 24 hours in Dulbecco's modified Eagle's medium with 2% fetal bovine serum.

Drug treatments. siRNAs formulated in phosphate-buffered saline (Sigma-Aldrich, St Louis, MO), poly I:C (InvivoGen, San Diego, CA), poly I:C_{12}U (Ampligen; Bioclones, Capetown, South Africa), lipopolysaccharide (InvivoGen), neutralizing rat antibodies against mouse TLR3 (eBioscience, San Diego, CA), isotype control IgGs (eBioscience) were dissolved in phosphate-buffered saline and injected into the vitreous cavity in a total volume of 1 µl. For RIG-I studies, *in vivo* transfection of 3p-RNA (1 µg) was performed using 10% NeuroPORTER (Genlantis, San Diego, CA). phosphate-buffered saline and poly I:C controls were also prepared. Subretinal injections (1 µl) in mice were performed using a Pico-Injector (PLI-100; Harvard Apparatus, Holliston, MA). For systemic studies, intravenous injections of poly I:C (100–300 µg) or serum stable 21-nt-*Luc*-siRNA (100 µg) were administered by tail vein on day 0, 3, and 7.

siRNA. Chemical siRNA sequences and modifications are listed in **Supplementary Table S1**. All siRNAs were purchased from Dharmacon, Lafayette, CO.

Fundus photography. Retinal photographs of dilated mouse eyes were taken with a TRC-50 IX camera (Topcon, Tokyo, Japan) coupled with a 3CCD digital color imaging system (Sony, Tokyo, Japan) and processed identically in Photoshop CS4 (Adobe Systems, San Jose, CA).

Image acquisition and processing. All bright field and fluorescent microscopy images were acquired on a Zeiss Axio Observer Z1 microscope with 10×/0.3, 20×/0.8, or 63×/1.40 objectives with a color ICcR3 camera using Axiovision software (Carl Zeiss, Thornwood, NY). Sections were mounted in Aqueous or Vector Mount (Vector Labs, Burlingame, CA) for bright field and fluorescent imaging, respectively. Images were then exported as TIFF files to Photoshop CS4 (Adobe Systems) and identically processed for gamma adjustments.

Electroretinography. Mice were dark adapted overnight, anesthetized, and both eyes were positioned within a ColorBurst Ganzfeld stimulator (E2; Diagnosys, Lowell, MA). After placing corneal and ground electrode, Espion software (Diagnosys) was used to deliver a fully automated flash intensity series from which retinal responses were recorded. Maximal a- and b-wave values were identified for each flash intensity, and mean values were compared for statistical analysis.

Optical coherence tomography. Mice were anesthetized, and eyes were imaged using a commercially available spectral domain OCT fitted with a 30° lens (Spectralis; Heidelberg Engineering, Heidelberg, Germany). Spectral domain optical coherence tomography imaging was done in the same session as cSLO to minimize variability. For OCT imaging, we used a commercially available Spectralis HRA+OCT device from Heidelberg Engineering featuring a broadband superluminescent diode at $\lambda = 870$ nm as low coherent light source. Two-dimensional B-scans were acquired at a speed of 40,000 scans per second with a tracking infrared laser to reduce speckle noise from eye movements.

Histology. Mouse eyes were enucleated and fixed with 4% paraformaldehyde/3.5% glutaraldehyde, postfixed in 2% osmium tetroxide, and dehydrated in ethanol and embedded. Semithin (1 µm) sections were cut and stained with toluidine blue.

TUNEL immunohistochemistry. Tissue sections were prepared and treated according to manufacturer's recommendations (TACS XL; Trevigen, Gaithersburg, MD).

Transmission electron microscopy. Uranyl acetate and lead citrate stained ultrathin sections were prepared for imaging with transmission electron microscope (Biotwin 12; Philips, Amsterdam, the Netherlands).

RPE morphology. Mouse RPE/choroid flat mounts were prepared, fixed with 100% MeOH and blocked overnight in 1% bovine serum albumin in phosphate-buffered saline with 0.05% Triton-X at 4°C. Flat mounts were then incubated with rabbit antibodies against zonula occludens-1 (1:100; Invitrogen, Carlsbad, CA) overnight followed by washing and fluorescent secondary antibody (AF594, 1:1,000; Invitrogen) for 3 hours. RPE flat mounts were imaged on an AxioObserver Z1 fluorescent microscope (Carl Zeiss).

Western blotting. Cells were homogenized in lysis buffer (10 mmol/l Tris base, pH 7.4, 150 mmol/l NaCl, 1 mmol/l EDTA, 1 mmol/l EGTA, 1% Triton X-100, 0.5% NP-40, protease and phosphatase inhibitor cocktail (Roche, Basel, Switzerland)). Protein concentrations were determined using a Bradford assay kit (Bio-Rad, Hercules, CA) with bovine serum albumin as a standard. Proteins (40–100 µg) were run on 4–12% Novex Bis–Tris gels (Invitrogen). The transferred membranes were blocked for 1 hour at room temperature and incubated with primary antibodies at 4 °C overnight. The secondary antibodies were used (1:5,000) for 1 hour at room temperature. The signal was visualized by enhanced chemiluminescence (ECL plus; Pierce, Rockford, IL) and captured by VisionWorksLS Image Acquisition and Analysis software (Version 6.7.2, UVP; LLC, Upland, CA).

Viability assay for hRPE cells. Confluent early passage hRPE cell isolates were synchronized by overnight serum starvation. Ninety six-well plates

were seeded at a density of 10,000 cells/well, followed by stimulation for 24 hours with interferon-α/β (1,000 U/ml; PBL InterferonSource). Cultures were then treated with polyinosine–polycytidylic acid (high-molecular weight poly I:C; InvivoGen), serum stable 21-nt-*Luc*-siRNA, or serum stable 16-nt-*Luc*-siRNA. At 48 hours, cell viability was measured with a bromodeoxyuridine enzyme-linked immunosorbent assay (Chemicon, Billerica, MA) according to manufacturer's instructions. Optical densities were analyzed at 450 nm (Synergy 4; BioTek, Winooski, VT).

Flow cytometry for surface and intracellular TLR3 on RPE. For surface TLR3 staining, hRPE cells were treated with FcR block (BD, San Jose, CA) and incubated with PE-conjugated antihuman TLR3 (20 µg/ml; Imgenex, San Diego, CA). For intracellular TLR3 staining, cells were fixed and permeabilized with Leucoperm (Serotec, Raleigh, NC) and stained for TLR3 in the presence of 10% mouse serum. PE-conjugated mouse IgGκ1 isotype served as control (BD). A minimum of 10,000 events were acquired (LSRII; BD) and analyzed with Kolmogorov–Smirnov statistics (FlowJo; Tree Star, Ashland, OR).

Suspensions of C57BL/6J RPE/choroid cells (10^6) were isolated and incubated with APC anti-mouse CD31 antibody (20 µg/ml; BD) and PE anti-mouse CD147 antibody (20 µg/ml; eBioscience) to identify $CD147^+$ $CD31^-$ RPE cells. For surface TLR3 staining, cells were incubated with anti-mouse TLR3 (10 µg/ml; R&D Systems, Minneapolis, MN) that was preconjugated to Alexa Fluor 488 (Invitrogen). For intracellular TLR3 staining, CD31/CD147 labeled cells were subjected to fixation and permeabilization followed by incubation with anti-mouse TLR3 (5 µg/ml). Fluorescein isothiocyanate-conjugated rat IgG2a isotype (BD) served as a control. A minimum of 50,000 events were acquired (LSRII; BD) and analyzed with Kolmogorov–Smirnov statistics (FlowJo).

TLR3 localization by immunofluorescent microscopy. C57BL/6J mouse eye sections (10 µm) were fixed in ice-cold acetone for 10 minutes at 4 °C, blocked, and incubated with rabbit anti-mouse TLR3 (1:50; Imgenex) overnight at 4 °C followed by Alexa Fluor 594 goat anti-rabbit IgG (1:200; Invitrogen). For colabeling of RPE, sections were incubated with mouse anti-mouse RPE65 (1:50; Novus, Littleton, CO) followed fluorescein isothiocyanate staining using a mouse-on-mouse kit per manufacturer's recommendations (Vector, Burlingame, CA). Isotype controls (rabbit/mouse IgG; Jackson ImmunoResearch, Westgrove, PA) were processed in parallel. Images were acquired on an Axio Observer Z1 fluorescent microscope (Carl Zeiss).

TLR3 phosphorylation assay. Protein lysates from hRPE cells treated with 21-nt-Luc-siRNA, were separated by sodium dodecyl sulfate/polyacrylamide gel electrophoresis, followed by western blotting with anti-phospho-TLR3 antibody (pY759; Imgenex). GAPDH served as control for equal loading.

siRNA-TLR3 immunoprecipitation. Recombinant hTLR3 (rhTLR3) and biotinylated 21-nt-*Luc*-siRNA were mixed and treated by UV (Spectrolinker; Spectroline, Westbury, NY) for 30 minutes. To detect crosslinked siRNA–rhTLR3 complex, streptavidin immunoprecipitation was performed followed by western blotting with TLR3 antibody (315A; Imgenex). Competition assays used excessive (×10) nonbiotinylated 21-nt-*Luc*-siRNA.

IRF3 nuclear translocation. Immunoblots of total protein (80 µg) isolated from cytoplasmic and nuclear fractions of hRPE 1 hour after 21-nt-*Luc*-siRNA were incubated with primary antibodies (interferon regulatory factor-3; Cell Signaling, Danvers, MA; Nucleolin, Sigma; Vinculin, Santa Cruz Biotechnology, Santa Cruz, CA) at 4 °C overnight. Horseradish peroxidase coupled secondary antibodies were visualized by enhanced chemiluminescence (ECL plus). Images were captured by VisionWorksLS Image Acquisition (UVP).

Cleaved caspase-3 quantification and localization

Immunohistochemistry: Albino Balb/C mouse eyes ($n = 3$ per group) were embedded in medium (OCT) and snap-frozen in liquid nitrogen after enucleation. Cryosections (10 µm) were fixed with 2% PFA for 10 minutes, followed by incubation with 1% H_2O_2, 2% sodium azide, 0.1% saponin, 10 mmol/l HEPES in Earle's balanced salt solution (EBSS-saponin) for 1 hour. After blocking (Dako USA, Carpinteria, CA), sections incubated with primary antibody (1:100; Cell Signaling, Danvers, MA) in EBSS-saponin overnight at room temperature. After washing, detection was performed with a biotinylated secondary antibody (1:200; Vector Labs) for 30 m, avidin-peroxidase incubation (ABC; Vector) for 30 m and colorimetric staining (DAB, Vector).

Fluorometric plate assay: One hundred microgram of total protein was assayed for capsase-3 cleavage by a commercial kit (R&D Systems) and analyzed on fluorescent plate reader per manufacturer's recommendations (Synergy 4; BioTek).

Statistical analyses. Data analyzed with JMP 8.0 (SAS Software, Cary, NC) and expressed as mean ± SEM. Statistical significance was determined using Mann–Whitney *U*, Kruskal–Wallis or Fisher's exact test with $P < 0.05$.

SUPPLEMENTARY MATERIAL

Figure S1. TLR3 agonists and 21-nt-siRNAs uniformly induce retinal degeneration.
Figure S2. Cell permeant 21-nt-siRNAs are also retinotoxic.
Figure S3. Intraocular delivery is required for retinotoxicity.
Figure S4. 21-nt-*Luc*-siRNA-induced retinal degeneration suppresses GFP signal.
Figure S5. dsRNA-induced retinal degeneration does not require the alternate cytoplasmic sensor, RIG-I.
Figure S6. dsRNA-induced retinal degeneration does not require the alternate cytoplasmic sensors, MDA5 or PKR.
Figure S7. Histologic, ultrastructural, and functional rescue of 21-nt-siRNA-induced retinal degeneration in IRF3 deficient mice.
Table S1. siRNA sequences and modifications.

ACKNOWLEDGMENTS

We thank R. King, L. Xu, M. McConnell, C. Payne, G.R. Pattison, D. Robertson, and G. Botzet for technical assistance, and R. Mohan, P.A. Pearson, A.M. Rao, G.S. Rao, K. Ambati, and B. Savage for discussions. J.A. was supported by National Eye Institute/National Institutes of Health (NIH) grants R01EY018350, R01EY018836, R01EY020672, R21EY019778, RC1EY020442, the Doris Duke Distinguished Clinical Scientist Award, the Burroughs Wellcome Fund Clinical Scientist Award in Translational Research, the Dr E. Vernon Smith and Eloise C. Smith Macular Degeneration Endowed Chair, the Senior Scientist Investigator Award [Research to Prevent Blindness (RPB)], and a departmental unrestricted grant from the RPB; M.E.K. by NIH K08EY021757 and Foundation Fighting Blindness; J.Z.B. by NIH K08EY021521 and American Health Assistance Foundation; M.E.K. and J.Z.B. by University of Kentucky Physician Scientist Awards and International Retinal Research Foundation; S.B. and B.J.F. by NIH T32HL091812; B.K.A. by NIH R01EY017182, R01EY017950, VA Merit Award and Department of Defense; J.A. is named as an inventor on a patent application filed by the University of Kentucky on ultrashort siRNAs as TLR3 antagonists.

REFERENCES

1. Kaiser, PK, Symons, RC, Shah, SM, Quinlan, EJ, Tabandeh, H, Do, DV *et al.*; Sirna-027 Study Investigators. (2010). RNAi-based treatment for neovascular age-related macular degeneration by Sirna-027. *Am J Ophthalmol* **150**: 33–39.e2.
2. Kleinman, ME, Yamada, K, Takeda, A, Chandrasekaran, V, Nozaki, M, Baffi, JZ *et al.* (2008). Sequence- and target-independent angiogenesis suppression by siRNA via TLR3. *Nature* **452**: 591–597.
3. Ashikari, M, Tokoro, M, Itaya, M, Nozaki, M and Ogura, Y (2010). Suppression of laser-induced choroidal neovascularization by nontargeted siRNA. *Invest Ophthalmol Vis Sci* **51**: 3820–3824.
4. Gu, L, Chen, H, Tuo, J, Gao, X and Chen, L (2010). Inhibition of experimental choroidal neovascularization in mice by anti-VEGFA/VEGFR2 or non-specific siRNA. *Exp Eye Res* **91**: 433–439.
5. Bergé, M, Bonnin, P, Sulpice, E, Vilar, J, Allanic, D, Silvestre, JS *et al.* (2010). Small interfering RNAs induce target-independent inhibition of tumor growth and vasculature remodeling in a mouse model of hepatocellular carcinoma. *Am J Pathol* **177**: 3192–3201.

6. Alexopoulou, L, Holt, AC, Medzhitov, R and Flavell, RA (2001). Recognition of double-stranded RNA and activation of NF-kappaB by Toll-like receptor 3. *Nature* **413**: 732–738.
7. Kumar, MV, Nagineni, CN, Chin, MS, Hooks, JJ and Detrick, B (2004). Innate immunity in the retina: Toll-like receptor (TLR) signaling in human retinal pigment epithelial cells. *J Neuroimmunol* **153**: 7–15.
8. Yamamoto, M, Sato, S, Hemmi, H, Hoshino, K, Kaisho, T, Sanjo, H *et al.* (2003). Role of adaptor TRIF in the MyD88-independent toll-like receptor signaling pathway. *Science* **301**: 640–643.
9. Oshiumi, H, Matsumoto, M, Funami, K, Akazawa, T and Seya, T (2003). TICAM-1, an adaptor molecule that participates in Toll-like receptor 3-mediated interferon-β induction. *Nat Immunol* **4**: 161–167.
10. Yamamoto, M, Sato, S, Mori, K, Hoshino, K, Takeuchi, O, Takeda, K *et al.* (2002). Cutting edge: a novel Toll/IL-1 receptor domain-containing adapter that preferentially activates the IFN-β promoter in the Toll-like receptor signaling. *J Immunol* **169**: 6668–6672.
11. Kato, H, Takeuchi, O, Mikamo-Satoh, E, Hirai, R, Kawai, T, Matsushita, K *et al.* (2008). Length-dependent recognition of double-stranded ribonucleic acids by retinoic acid-inducible gene-I and melanoma differentiation-associated gene 5. *J Exp Med* **205**: 1601–1610.
12. Hornung, V, Ellegast, J, Kim, S, Brzózka, K, Jung, A, Kato, H *et al.* (2006). 5′-Triphosphate RNA is the ligand for RIG-I. *Science* **314**: 994–997.
13. Karikó, K, Bhuyan, P, Capodici, J and Weissman, D (2004). Small interfering RNAs mediate sequence-independent gene suppression and induce immune activation by signaling through toll-like receptor 3. *J Immunol* **172**: 6545–6549.
14. Pirher, N, Ivicak, K, Pohar, J, Bencina, M and Jerala, R (2008). A second binding site for double-stranded RNA in TLR3 and consequences for interferon activation. *Nat Struct Mol Biol* **15**: 761–763.
15. Lee, HK, Dunzendorfer, S, Soldau, K and Tobias, PS (2006). Double-stranded RNA-mediated TLR3 activation is enhanced by CD14. *Immunity* **24**: 153–163.
16. Kang, DC, Gopalkrishnan, RV, Wu, Q, Jankowsky, E, Pyle, AM and Fisher, PB (2002). mda-5: An interferon-inducible putative RNA helicase with double-stranded RNA-dependent ATPase activity and melanoma growth-suppressive properties. *Proc Natl Acad Sci USA* **99**: 637–642.
17. Yang, Z, Stratton, C, Francis, PJ, Kleinman, ME, Tan, PL, Gibbs, D *et al.* (2008). Toll-like receptor 3 and geographic atrophy in age-related macular degeneration. *N Engl J Med* **359**: 1456–1463.
18. Gowen, BB, Wong, MH, Jung, KH, Sanders, AB, Mitchell, WM, Alexopoulou, L *et al.* (2007). TLR3 is essential for the induction of protective immunity against Punta Toro Virus infection by the double-stranded RNA (dsRNA), poly(I:C12U), but not Poly(I:C): differential recognition of synthetic dsRNA molecules. *J Immunol* **178**: 5200–5208.
19. Soutschek, J, Akinc, A, Bramlage, B, Charisse, K, Constien, R, Donoghue, M *et al.* (2004). Therapeutic silencing of an endogenous gene by systemic administration of modified siRNAs. *Nature* **432**: 173–178.
20. Bird, AC, Bressler, NM, Bressler, SB, Chisholm, IH, Coscas, G, Davis, MD *et al.* (1995). An international classification and grading system for age-related maculopathy and age-related macular degeneration. The International ARM Epidemiological Study Group. *Surv Ophthalmol* **39**: 367–374.
21. Matsumoto, M, Funami, K, Tanabe, M, Oshiumi, H, Shingai, M, Seto, Y *et al.* (2003). Subcellular localization of Toll-like receptor 3 in human dendritic cells. *J Immunol* **171**: 3154–3162.
22. Cho, WG, Albuquerque, RJ, Kleinman, ME, Tarallo, V, Greco, A, Nozaki, M *et al.* (2009). Small interfering RNA-induced TLR3 activation inhibits blood and lymphatic vessel growth. *Proc Natl Acad Sci USA* **106**: 7137–7142.
23. Pegu, A, Qin, S, Fallert Junecko, BA, Nisato, RE, Pepper, MS and Reinhart, TA (2008). Human lymphatic endothelial cells express multiple functional TLRs. *J Immunol* **180**: 3399–3405.
24. Bell, JK, Botos, I, Hall, PR, Askins, J, Shiloach, J, Segal, DM *et al.* (2005). The molecular structure of the Toll-like receptor 3 ligand-binding domain. *Proc Natl Acad Sci USA* **102**: 10976–10980.
25. Ranjith-Kumar, CT, Miller, W, Xiong, J, Russell, WK, Lamb, R, Santos, J *et al.* (2007). Biochemical and functional analyses of the human Toll-like receptor 3 ectodomain. *J Biol Chem* **282**: 7668–7678.
26. Sarkar, SN, Smith, HL, Rowe, TM and Sen, GC (2003). Double-stranded RNA signaling by Toll-like receptor 3 requires specific tyrosine residues in its cytoplasmic domain. *J Biol Chem* **278**: 4393–4396.
27. Dogusan, Z, García, M, Flamez, D, Alexopoulou, L, Goldman, M, Gysemans, C *et al.* (2008). Double-stranded RNA induces pancreatic β-cell apoptosis by activation of the toll-like receptor 3 and interferon regulatory factor 3 pathways. *Diabetes* **57**: 1236–1245.
28. Seya, T and Matsumoto, M (2009). The extrinsic RNA-sensing pathway for adjuvant immunotherapy of cancer. *Cancer Immunol Immunother* **58**: 1175–1184.
29. Chang, B, Hawes, NL, Hurd, RE, Davisson, MT, Nusinowitz, S and Heckenlively, JR (2002). Retinal degeneration mutants in the mouse. *Vision Res* **42**: 517–525.
30. Sun, R, Zhang, Y, Lv, Q, Liu, B, Jin, M, Zhang, W *et al.* (2011). Toll-like receptor 3 (TLR3) induces apoptosis via death receptors and mitochondria by up-regulating the transactivating p63 isoform α (TAP63α). *J Biol Chem* **286**: 15918–15928.
31. Yu, M, Lam, J, Rada, B, Leto, TL and Levine, SJ (2011). Double-stranded RNA induces shedding of the 34-kDa soluble TNFR1 from human airway epithelial cells via TLR3-TRIF-RIP1-dependent signaling: roles for dual oxidase 2- and caspase-dependent pathways. *J Immunol* **186**: 1180–1188.
32. Salaun, B, Coste, I, Rissoan, MC, Lebecque, SJ and Renno, T (2006). TLR3 can directly trigger apoptosis in human cancer cells. *J Immunol* **176**: 4894–4901.
33. Chang, CI, Yoo, JW, Hong, SW, Lee, SE, Kang, HS, Sun, X *et al.* (2009). Asymmetric shorter-duplex siRNA structures trigger efficient gene silencing with reduced nonspecific effects. *Mol Ther* **17**: 725–732.
34. McLeod, DS, Grebe, R, Bhutto, I, Merges, C, Baba, T and Lutty, GA (2009). Relationship between RPE and choriocapillaris in age-related macular degeneration. *Invest Ophthalmol Vis Sci* **50**: 4982–4991.
35. Kaneko, H, Dridi, S, Tarallo, V, Gelfand, BD, Fowler, BJ, Cho, WG *et al.* (2011). DICER1 deficit induces Alu RNA toxicity in age-related macular degeneration. *Nature* **471**: 325–330.